

Enhancing flame retardancy properties of apricot kernel powder filled polypropylene

Merve Ekti¹, Sibel Aker¹, Mehmet Sarikanat², Lutfiye Altay*², Yoldas Seki³

¹İzmir Eğitim Sağlık Sanayi Yatırım A.Ş., Turgutlu, Manisa, Turkey

²Mechanical Engineering Department, Ege University, Bornova, Izmir, Turkey

³Faculty of Science, Dokuz Eylul University, Buca, Izmir, Turkey

ABSTRACT

In recent years, there has been growing interest in using agricultural waste in thermoplastic composites. This is due to the environmental benefits of such composites and their potential as sustainable alternatives to conventional mineral-filled thermoplastics. The aim of this study was to develop halogen-free flame-retardant polypropylene composites filled with apricot kernel shells, intended to replace conventional mineral-filled thermoplastic composites. Polypropylene-based composites with apricot kernel shells at varying weight percentages (10%, 20%, 30%, and 40%) were manufactured by a twin-screw extruder and an injection molding machine. The optimal filling ratio of 20% by weight was determined by analyzing the material's mechanical, thermal, and physical properties. Further improvement in the mechanical properties of composites, along with enhanced interaction between the filler and matrix, was achieved by adding 2% by weight of MAPP. Although the mechanical properties of the composites were significantly enhanced with the addition of 2 wt% compatibilizer, the thermal properties remained unchanged. The addition of a halogen-free flame retardant decreased the mechanical properties of the composites considerably, but it improved their thermal stability and horizontal flame-propagation speed. Compared to the 20 wt% apricot kernel shell-filled polypropylene composite without flame retardant, the incorporation of 5 wt% flame retardant resulted in a 33% reduction in burning rate.

Keywords: Flame retardance; polypropylene; apricot kernel; composites; agricultural waste.

INTRODUCTION

Since the latter part of the 20th century, composite materials have garnered significant interest in materials science and advanced technology. Industries such as aerospace, construction, automotive, sports, and biomedical extensively utilize these materials due to their superior mechanical and structural qualities, resistance to chemicals, and ability to withstand abrasions[1]. Thermoplastic composite materials are particularly notable for their low weight, high chemical resistance, ease of processing, and recyclability, making them especially valuable in the automotive industry[2]. These composites are often reinforced with a variety of fillers and polymeric matrices derived from petroleum. However, the synthetic nature of these reinforcements and resin systems raises environmental concerns. Consequently, researchers are focusing on the use of natural fillers and

reinforcements, along with bio-based or biodegradable resins, to develop greener and more environmentally friendly composite materials[3, 4].

Despite their potential, bio-based or biodegradable resins currently exhibit mechanical and thermal properties that are insufficient for certain applications, and their industrial production remains costly and limited. To address these challenges, numerous initiatives aim to enhance bio-resin production and replace conventional petroleum-derived resins. One promising approach to making composites more environmentally friendly involves the use of natural fibers or fillers, particularly agricultural wastes, which hold significant potential as natural fillers[5].

Bio-based additives are used to enhance the mechanical and chemical properties of thermoplastics. These additives include lignin, cellulose, starch, and polymers derived from various vegetable oils. Agricultural wastes such as rice husks, corn cobs, and cotton linters are significant sources of bio-based additives. Utilizing these wastes not only valorizes the materials but also mitigates environmental impacts[6]. However these natural additives are mainly composed of cellulose, hemicelluloses, lignin and other components, which impart the plant fiber with inherent flammability[7]. Few studies have investigated composite structures with high flame resistance made from natural fibers combined with halogen-free flame-retardant chemicals. Given that certain plastic parts in the automotive industry come into contact with cables and electronic components, enhancing combustion performance while meeting the criterion of lightness is essential. This approach also lowers the carbon footprint[8, 9].

Turkey is one of the leading countries in apricot production, leading to significant apricot kernel waste. Utilizing apricot kernel powder in plastic production holds substantial economic and environmental potential. This powder can be used as a filler in thermoplastic composites, enhancing the material's mechanical properties while contributing to waste management [10]. The use of a locally abundant resource like apricot kernel not only enhances cost efficiency but also aids in valorizing agricultural waste in Turkey[11]

Studies on apricot kernel shell in thermoplastic matrices are very limited, and to the best of our knowledge, its use in flame-retardant polypropylene systems has not been previously reported. While many studies examine mechanical reinforcement of PP with lignocellulosic fillers, significantly fewer studies address flame retardancy in such systems, particularly using halogen-free phosphorus-based additives. In this study, we specifically investigate how apricot kernel shell powder as an agricultural waste interacts with a nitrogen–phosphorus-based flame retardant and how this combination affects horizontal burning behavior (UL-94 HB), thermal stability, thermomechanical performance, crystallization behavior.

EXPERIMENTAL

Materials

Polypropylene copolymer with the trade name 49MK45 was supplied by Sabic Industries Corporation (Saudi Arabia). The filler material used was apricot kernel shell powder with a particle size of 100 μm , which was provided by Tersun Apricot Kernel Processing Industry (Turkey). The halogen-free flame retardant (FR) additive, with the trade name EPFR-100A and based on nitrogen and phosphate, was purchased from Presafer Phosphor Chemical Co. Ltd. (China). In order to improve the compatibility between the filler and the polymeric matrix, a compatibilizer containing maleic anhydride grafted polypropylene (MAPP), trade name Licocene 7452, was supplied by Clariant AG (Switzerland).

Production of Composites

This study was carried out in two stages. In the first stage, PP composites filled with apricot kernel shell (K) at varying ratios of 10%, 20%, 30% and 40% by weight were produced and characterized to examine the effect of varying filler ratio. Based on physical, thermal, and mechanical properties, a 20 wt% filler ratio was chosen as optimal, and 2% MAPP was added to the PP composite to enhance the interaction between the filler and the matrix. In the second stage, FR additives were added at 5 wt%, 10 wt%, 15 wt% and 20 wt% to improve the flame retardancy performance of apricot kernel shell filled PP based composites, and their physical, mechanical, thermal and flame retardancy properties were analyzed. Specimen codes and their composition are shown in Table 1.

Table 1. Specimen codes and their compositions.

Specimen Codes	Composition (%)			
	PP	K	MAPP	FR
10K	90	10	0	0
20K	80	20	0	0
30K	70	30	0	0
40K	60	40	0	0
20K-2MAPP	78	20	2	0
20K-2MAPP-5FR	73	20	2	5
20K-2MAPP-10FR	68	20	2	10
20K-2MAPP-15FR	63	20	2	15
20K-2MAPP-20FR	58	20	2	20

All composite materials were produced using Leistritz Extruder Corporation twin screw extruder, ZSE 27 MAXX model, with a screw diameter of 27 mm and an L/D ratio of 48, rotating in the same direction. Test specimens for characterizing the produced PP composite granules were prepared using a Bole injection molding machine, BL90EK model. Injection molding conditions for each test sample were kept constant throughout the injection process.

Characterization methods

Density measurement

The densities of the composites were determined using a Kern brand MD-200S model density meter, following the ISO 1183-1 standard. The density of each composite was measured three times, and the average was recorded.

Melt flow index (MFI)

MFI measurements of the composites were performed using a Göttfert Melt indexer mi2.2. The measurements were carried out at a melt temperature of 230°C and a piston load of 2.16 kg, following the ISO 1133-1 standard.

Tensile test

A Hegewald-Peschke Inspect 20 tensile strength testing machine, equipped with a video extensometer system, was used to assess the mechanical strength of the composites according to ISO 527 standard. The tensile strength of the specimens was measured at room temperature with a test speed of 50 mm/min and a 20 kN load cell. At least five repetitions were conducted for each sample, and average values were calculated.

Flexural test

The flexural characteristics of PP composites were assessed using the ISO 178 standard. A Hegewald & Peschke Inspect 20 universal testing machine was utilized to conduct the bending test at room temperature. The crosshead speed was set to 2 mm/min, and the span length was 32 mm. Five repetitions were conducted for each sample, and average values were calculated.

Impact strength test

The Instron brand device was utilized to test the impact strength, following the procedures outlined in the ISO 180 standard at room temperature. Each measurement was repeated three times, and the average result was recorded.

Heat deflection temperature (HDT) test

The HDT values of PP composites were determined using a Coesfeld brand HDT-Vicat Testing Instrument in accordance with the ISO 75 standard. The standard pressure was set at 1.8 MPa, and the heating rate was maintained at 120 K/h.

Vicat softening temperature (VST) test

The VST values were determined in accordance with ISO 305 standard, employing a 50 N load and a heating rate of 120 K/h.

Differential scanning Calorimetry (DSC) analysis

DSC analysis of the samples was performed using a TA Instruments Inc. DSCQ20 model device. The specimens were initially equilibrated at 300°C, then cooled to a final temperature of -80°C at a rate of 10 °C/min. Subsequently, the specimens were heated from -80°C to 300°C at a heating rate of 10°C/min. The crystallinity of the materials was then calculated using the following equation based on the results obtained from the DSC analysis.

$$X_c(\%) = \frac{\Delta H_m}{(1 - y)\Delta H_{0m}} \times 100$$

where X_c denotes the crystallinity, ΔH_m represents the enthalpy of the samples (J/g), y indicates the weight ratio of filler/additive. ΔH_m^0 is the enthalpy of melting of PP with 100% crystallinity (ΔH_m^0 : 207 J/g)[12].

Thermogravimetric (TG) analysis

TG analysis of the composites was performed using a TGA-Q50 instrument from TA Instruments Inc. The heating process was carried out at a heating rate of 10°C/min under a nitrogen atmosphere, up to 800°C.

UL-94 horizontal burning test

An Atlas brand HVUL-2 model horizontal and vertical flammability analyzer was utilized to determine the flame-retardant properties of the composites. The tests were conducted in accordance with the UL94-HB Standard, measuring the flame speed of specimens that were 125 mm long, 3 mm wide, and 3 mm thick, after exposure to a fixed flame source at a 45° angle for 30 s. The material was marked at intervals of 25 mm, 75 mm and 25 mm, and the time taken to burn the remaining portion after the first 25 mm was ignited served as the basis for analysis.

Scanning electron microscopy (SEM) analysis

A Scanning Electron Microscope (SEM, Carl Zeiss 300VP, Germany) was employed to characterize the morphological changes of composites. Prior to SEM observations, fractured surfaces of the samples were coated with a thin layer of gold using plasma sputtering apparatus. All SEM images presented in this study were obtained from tensile fracture surfaces of specimens tested according to ISO 527.

RESULTS AND DISCUSSION

Density

The density values are given in **Error! Reference source not found.** From the lowest to the highest filler ratio with PP, the densities of composites were determined to be 0.91 g/cm³, 0.92 g/cm³, 0.95 g/cm³, 0.96 g/cm³, and 0.98 g/cm³, respectively. As expected, there were no significant differences in density

values as the filling ratio increased due to the low density of the apricot kernel shell. This finding is consistent with the results of earlier research that have been published in the literature [13, 14]. The density of the composites remained unaffected after the addition of MAPP. However, the density of the composites increased with the addition of FR additive. Density also serves an indication that the additive can be accurately added to the composite with minimum loss.

Table 2. Density values of PP composites.

Specimen Name	Density (g/cm ³)
PP	0.91 ± 0.01
10K	0.92 ± 0.01
20K	0.95 ± 0.00
30K	0.96 ± 0.01
40K	0.98 ± 0.01
20K-2MAPP	0.96 ± 0.01
20K-2MAPP-5FR	0.98 ± 0.01
20K-2MAPP-10FR	1.02 ± 0.01
20K-2MAPP-15FR	1.04 ± 0.01
20K-2MAPP-20FR	1.09 ± 0.01

Melt flow index

MFI values of PP composites were measured, and the results are shown in Figure 1. As the filler content increased, the MFI value decreased. Since MFI is a measure of material viscosity, the decrease in MFI value can be attributed to the increasing viscosity. As the filler ratio increased, the movement of thermoplastic polymer chains became more difficult, resulting in an increase in the material's viscosity[15]. The addition of MAPP and FR additives did not cause a significant change in MFI. However, a high FR loading of 20wt% restricted the movement of the polymer chains, leading to a decrease in the MFI value[16].

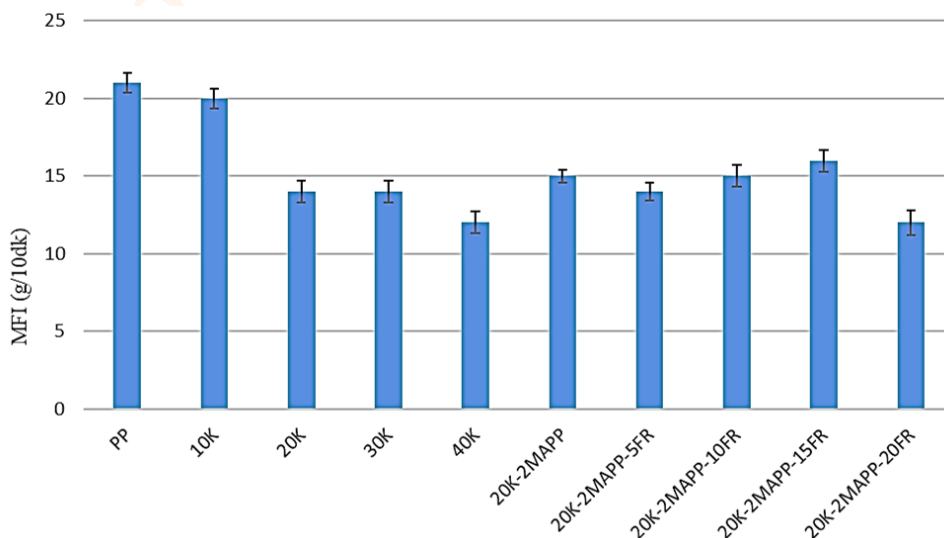


Figure 1. MFI values of PP composites.

Mechanical properties

Tensile strength

Tensile properties of PP and its composites are presented in **Error! Reference source not found.** It was observed that the tensile strength of PP composites filled with apricot kernel shell powder decreased with increasing the filler content. The highest tensile strength was obtained in 10K composite with 18.1 MPa, and the lowest tensile strength was obtained in 40K composite with 13.6 MPa. Increasing the filler ratio increases the interaction between particles and causes an increase in the stress concentration in the matrix, resulting in uneven stress distributions. Thus, the material is unable to evenly distribute the loads applied to it. Since tensile strength is a measure of the maximum force that the material can withstand under a tensile test, a decrease in tensile strength is expected [17, 18]. The moduli of elasticity values of PP, 10K, 20K, 30K, 40K were obtained to be 1521 MPa, 1652 MPa, 1851 MPa, 1902 MPa, 2004 MPa, respectively. It was observed that the highest modulus of elasticity value was obtained in the 40K composite, and the moduli of elasticity of the materials generally tended to increase with increasing filler ratio [19-21]. The addition of MAPP increased the tensile strength of the composite and showed a significant improvement compared to the 20K composite without compatibilizer. It was observed that the tensile strength increased due to the compatibilizer improves the filler-matrix interface [22]. Examination of the tensile strength results revealed that noticeable difference cannot be observed until 10 wt% FR loading. However, when the FR ratio increased to 20wt%, a comparatively significant loss in tensile strength was reported in this study. The 20K-2MAPP-20FR composite has shown the lowest tensile strength (19.5 MPa). Due to a loss of matrix homogeneity caused by high amounts of FR additives, the tensile strength was reduced [23, 24]. It can be concluded that there is an increasing trend in the modulus of elasticity because of the rising FR ratio, which makes composite materials stiffer and less capable of flexing under stress-strain pressures [25].

Table 3. Mechanical properties of PP composites.

Composition	Tensile Strength (MPa)	Elastic Modulus (MPa)	Flexural Strength (MPa)	Flexural Modulus (MPa)	Izod Notched Impact Strength (kJ/m ²)
PP	24.6 ± 0.2	1521 ± 77	28.2 ± 0.2	762 ± 34	6.0 ± 0.0
10K	18.1 ± 0.1	1652 ± 46	27.8 ± 0.2	891 ± 54	5.3 ± 0.6
20K	17.2 ± 0.3	1851 ± 62	32.4 ± 0.5	1275 ± 71	4.8 ± 0.9
30K	17.1 ± 0.2	1902 ± 89	33.8 ± 0.2	1634 ± 46	3.6 ± 0.3
40K	13.6 ± 0.3	2004 ± 102	24.6 ± 0.4	1801 ± 91	3.3 ± 0.6
20K-2MAPP	21.8 ± 0.2	1602 ± 92	42.1 ± 0.7	1562 ± 45	6.1 ± 0.6
20K-2MAPP-5FR	21.7 ± 0.5	1982 ± 82	35.4 ± 0.1	1756 ± 82	7.0 ± 0.0
20K-2MAPP-10FR	22.3 ± 0.0	2254 ± 95	35.6 ± 0.4	1999 ± 91	6.0 ± 0.0
20K-2MAPP-15FR	21.4 ± 0.5	2673 ± 78	37.8 ± 0.4	2391 ± 87	6.0 ± 0.0
20K-2MAPP-20FR	19.5 ± 1.7	3267 ± 101	36.0 ± 0.1	2651 ± 53	5.0 ± 0.0

Flexural properties

When examining the flexural strength of the composites, it is observed that it increases up to a 30 wt% filler reinforcement, but then begins to decrease. As explained in the literature, this phenomenon occurs because the filler is homogeneously dispersed in the matrix, enhancing its interaction with the matrix and thereby increasing the material's load-bearing capacity under bending, leading to an increase in flexural strength[26]. However, with further increases in filler ratio, the flexibility of the material decreases, along with its resistance to bending forces, resulting in a subsequent decrease in flexural strength. Moreover, as the filler ratio increases, the stiffness of the material, and consequently the flexural modulus values, also increase[27]. MAPP addition into the composites increased the flexural strength and modulus by increasing the interaction between the filler and the polymer. Upon analysis of the flexural strength values (Table 3), it is observed that it tends to increase slightly up to 15% flame retardant additive loading after which it starts to decrease at higher loadings. Although not significant, this increase can be attributed to the flame retardant additive, which renders the structure of the polymeric matrix more rigid, thereby reducing the material's flexibility under applied bending forces[28].

Impact strength

As can be seen from Table 3, notched impact strength values of filled composites decreased compared to that of PP. The decrease in impact strength with an increase in the filler ratio is explained in the literature as the material starts to lose its flexibility due to the increase in stress within the matrix. Consequently, its capacity to absorb impact energy decreases, making it more brittle[27, 29]. The addition of MAPP improved the impact resistance as well as other mechanical properties. This indicates that the compatibility between the matrix and filler enhances the interface and increases the ability of the composites to absorb energy against an external force. As the FR ratio increased, the impact strength of PP composites decreased. This can be explained by the FR additive decreasing the efficiency of the matrix interface. Similar to Khairiah and Amamer's (2010) study, the 20K-2MAPP-20FR composite with 20% FR had the lowest impact strength[30]. The 20K-2MAPP composite without FR had the highest notched-impact strength value (7.0 kJ/m²).

HDT-VST

HDT and VST values of PP and its composites are presented in Table 4. The results indicate that upon adding 30K into PP, both HDT and VST values of PP increased. It is generally known that fillers tend to increase the HDT and VST values due to their superior thermal stability compared to the matrix, thus improving their ability to maintain shape at elevated temperature. However, this enhancement directly depends on the interaction between the filler and the matrix. At 40 wt% filler content, HDT and VST decrease despite higher filler loading. This suggests that excessive filler content may lead to

matrix discontinuity, increased porosity and microvoid formation, and local stress concentration sites. The weakening of the matrix-filler interface at high filler ratios, the degradation of the filler's homogeneity in the matrix, and the reduction in heat conduction are the reasons for the decrease in HDT and VST values in 40K composite[31].The addition of a compatibilizer increased the HDT and VST values of composites. This can be explained by the fact that MAPP improves the bond between the filler and polymer matrix, resulting in a more rigid structure that may also possess better thermal properties[32].It was obtained that as the FR additive ratio increased, so did the HDT and VST values. The 20K-2MAPP-20FR composite has the highest HDT and VST values, indicating that the additional flame-retardant additive improves the composites' thermal stability and their capacity to withstand loads and high temperatures without deforming. Conversely, increasing the ratio of flame-retardant additive improves the composites' structural stability and increases the temperature at which the material begins to soften under load.

Table 4. HDT and VST values of PP composites.

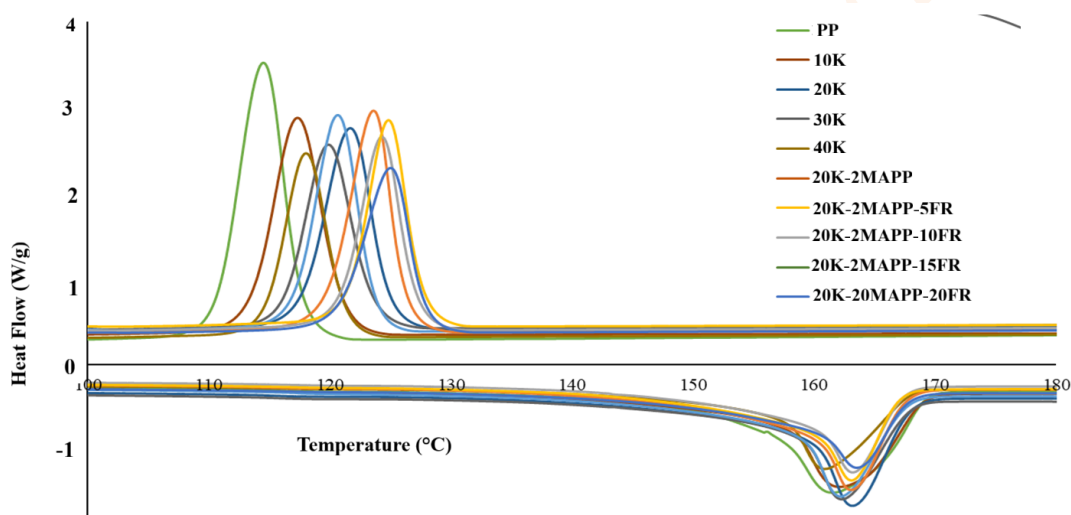
Specimen Name	HDT (°C)	VST (°C)
PP	65	82
10K	63	79
20K	65	80
30K	71	87
40K	68	69
20K-2MAPP	72	88
20K-2MAPP-5FR	61	83
20K-2MAPP-10FR	64	86
20K-2MAPP-15FR	70	87
20K-2MAPP-20FR	74	89

DSC analysis

Figure 2 shows DSC curves of both PP and its composites, and Table 5 summarizes the data collected from the DSC curves. As expected, changing the filler ratio and adding FR material did not lead to a significant change in the melting temperatures of the composites. It is known that fillers have minimal impact on the crystalline structure of the polymer and, consequently, on the melting behavior of the material. The melting temperature corresponds to the chemical structure of the polymer matrix[33].It was shown that as the FR loading ratio increased, the melting enthalpy of the composites decreased. This is expected because incorporation of FR modifies the polymer chains' crystal structure and reduces their interchain interaction. Compared to the 20K-2MAPP composite without FR, the crystallinity values of all composites with FR generally increased. This can be explained by the fact that the FR addition makes PP composites more thermally stable, allowing crystallization to occur at higher temperatures and resulting in higher crystallinity values.

Table 5. DSC data of PP composites.

Composition	T _m (°C)	ΔH _m (J/g)	T _c (°C)	ΔH _c (J/g)	X _c (%)
PP	162	85.8	115	95.2	41.5
10K	162	71.1	117	77.4	38.1
20K	163	62.9	122	68.6	38.0
30K	162	63.5	120	64.2	43.8
40K	161	52.3	118	56.3	42.1
20K-2MAPP	162	57.7	121	70.7	34.9
20K-2MAPP-5FR	163	62.4	124	67.6	40.7
20K-2MAPP-10FR	163	55.1	124	57.8	39.1
20K-2MAPP-15FR	163	49.9	125	59.9	38.3
20K-2MAPP-20FR	164	51.5	125	54.3	42.9

**Figure 2.** DSC curves of PP and its composites.

TG analysis

TGA curves and the data obtained from these curves are presented in Figure 3 and Table 6 respectively. As can be seen from Table 6, Neat PP exhibited a maximum degradation temperature (T_{max}) of 472°C and a temperature at 5% mass loss value ($T_{5\%}$) of 426°C, with nearly complete volatilization (99.8% total weight loss), which is consistent with the typical single-step thermal degradation behavior of PP under nitrogen atmosphere[34]. The incorporation of apricot kernel shell significantly influenced the initial thermal degradation of the composites. Although T_{max} values remained relatively close to that of neat PP at low filler loadings (for 10K, T_{max} = 472°C), a gradual decrease was observed at higher filler contents, decreasing 432°C for the 40K composite. This reduction can be ascribed to the presence of lignocellulosic components such as hemicellulose, cellulose, and lignin, which thermally decompose at lower temperatures (typically between 250–

350°C) compared to polypropylene[35]. Therefore, the early-stage degradation behavior of the composites is mainly governed by the thermal decomposition of the natural filler. This effect is more clearly reflected in the T5% values. A marked decrease in T5% was observed with increasing filler ratio, dropping from 426°C for neat PP to 321°C (10K), 272°C (30K), and 256°C (40K). These results confirm that the initial thermal stability of the composites decreases due to the earlier degradation of apricot kernel shell particles. The total weight loss decreased with increasing apricot kernel shell content, from 99.8% for neat PP to 92.7% for the 40K composite. There were no significant changes in the maximum mass losses due to increasing filler ratio[36]. As the FR loading increased to 20 wt%, T_{max} value increased from 463°C to 480°C. Additionally, the total mass loss significantly decreased, reaching 83.7% for the 20K-2MAPP-20FR composite. This behavior indicates enhanced char formation and improved thermal resistance at high temperatures. It can be reported that as the FR content increased, the total mass loss of the composites reduced. This can be attributed to the fact that FR additions enhance the materials' ability to burn by creating a char layer during combustion, which lowers mass losses[37].

Table 6. TGA data of PP and its composites.

Composition	T_{max} (°C)	Temperature at 5% weight loss (°C)	Total weight loss (%)
PP	472	426	99.8
10K	472	321	97.6
20K	461	383	96.6
30K	463	272	95.5
40K	432	256	92.7
20K-2MAPP	463	282	96.7
20K-2MAPP-5FR	476	286	91.2
20K-2MAPP-10FR	477	293	89.7
20K-2MAPP-15FR	479	292	85.2
20K-2MAPP-20FR	480	292	83.7

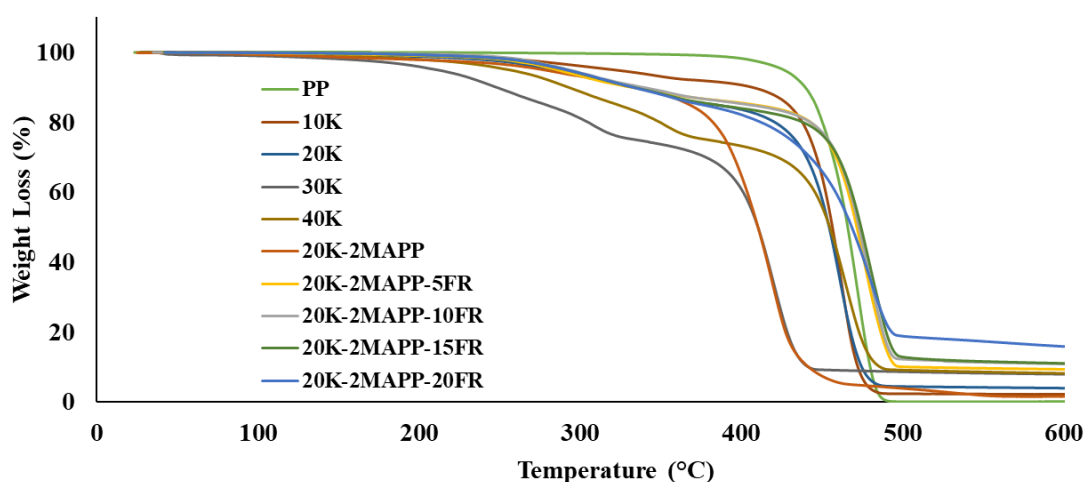


Figure 3. TGA curves of PP and its composites.

Horizontal burning test

The horizontal flame burning rate of PP and its composites were measured and the results are presented in Table 7. From the results, it was determined that the flame burning rate increased compared to PP due to the high flammability of apricot kernel shell, deviating from the HB flame retardancy class where it must be less than 40 mm/min. Performance improvement of 33% were reported for 20K-2MAPP and 20K-2MAPP-5FR composites upon the addition of FR additive. The ability of phosphorus-based flame retardant to create a stable char layer on the material's surface at high temperatures helps to explain this improvement. This layer of char acts as a barrier to reduce heat transfer and prevents the release of combustible gases. The addition of phosphorus-based flame retardant results in the formation of a char with a tendency to be carbonaceous and dense[38]. Consequently, the FR addition helped to improve the flame retardancy characteristics of the composites, which had declined compared to PP, improve, and reduced the rate at which flames spread. Pongsa et al. (2021) also added diammonium phosphate and TiO₂ to the composites produced using waste pineapple fibers and found that the horizontal flame propagation rates decreased, and combustion performances improved[39].

Table 7. Burning rate of flame-retardant PP and its composites.

Composition	Horizontal Flame Burning Rate (mm/min)
PP	28.0
20K	46.0
20K-2MAPP	49.3
20K-2MAPP-5FR	32.9
20K-2MAPP-10FR	32.1
20K-2MAPP-15FR	28.4
20K-2MAPP-20FR	27.5

SEM analysis

SEM images of apricot kernel shell-filled PP and halogen free FR loaded apricot kernel shell-filled PP composites are shown in **Error! Reference source not found.** and 5, respectively. For the 10K and 20K composites, the fracture surfaces exhibit relatively homogeneous filler dispersion with limited void formation. The matrix appears to partially wet the filler surfaces, although some micro-gaps and localized pull-out traces are visible, indicating moderate interfacial adhesion. As the filler loading increases to 30K and 40K, the fracture morphology becomes significantly rougher, and the presence of voids, agglomerated regions, and filler pull-out cavities becomes more pronounced. It can be reported that increasing the filling ratio leads to an increase in voids within the matrix and the formation of more irregular structures[40]. The incorporation of 2 wt% MAPP results in a visibly improved interfacial structure. The fracture surface of the 20K-2MAPP composite shows reduced interfacial gaps and fewer pull-out cavities compared to the non-compatibilized system. It can be noted that the

filler-matrix interface is improved by the compatibilizer. Consequently, SEM analysis shows that the gap between the filler and matrix decreases, resulting in a smoother surface and a more uniform interfacial appearance[41, 42]. At higher FR contents (15–20 wt%), the microstructure becomes more heterogeneous, with increased microvoids, and localized phase separation. It can be added that the addition of FR disrupts the homogeneity of the composites. Increased usage of FR additives results in defects on the surface such as cracks, roughness, and voids[43].

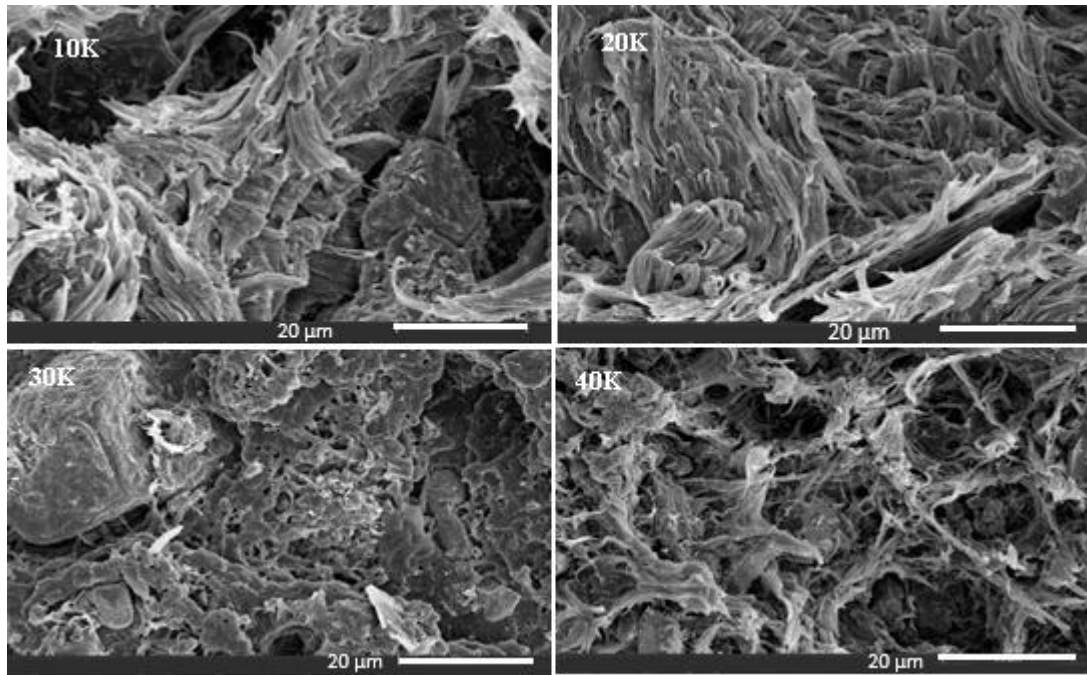


Figure 4. SEM images of PP composites.

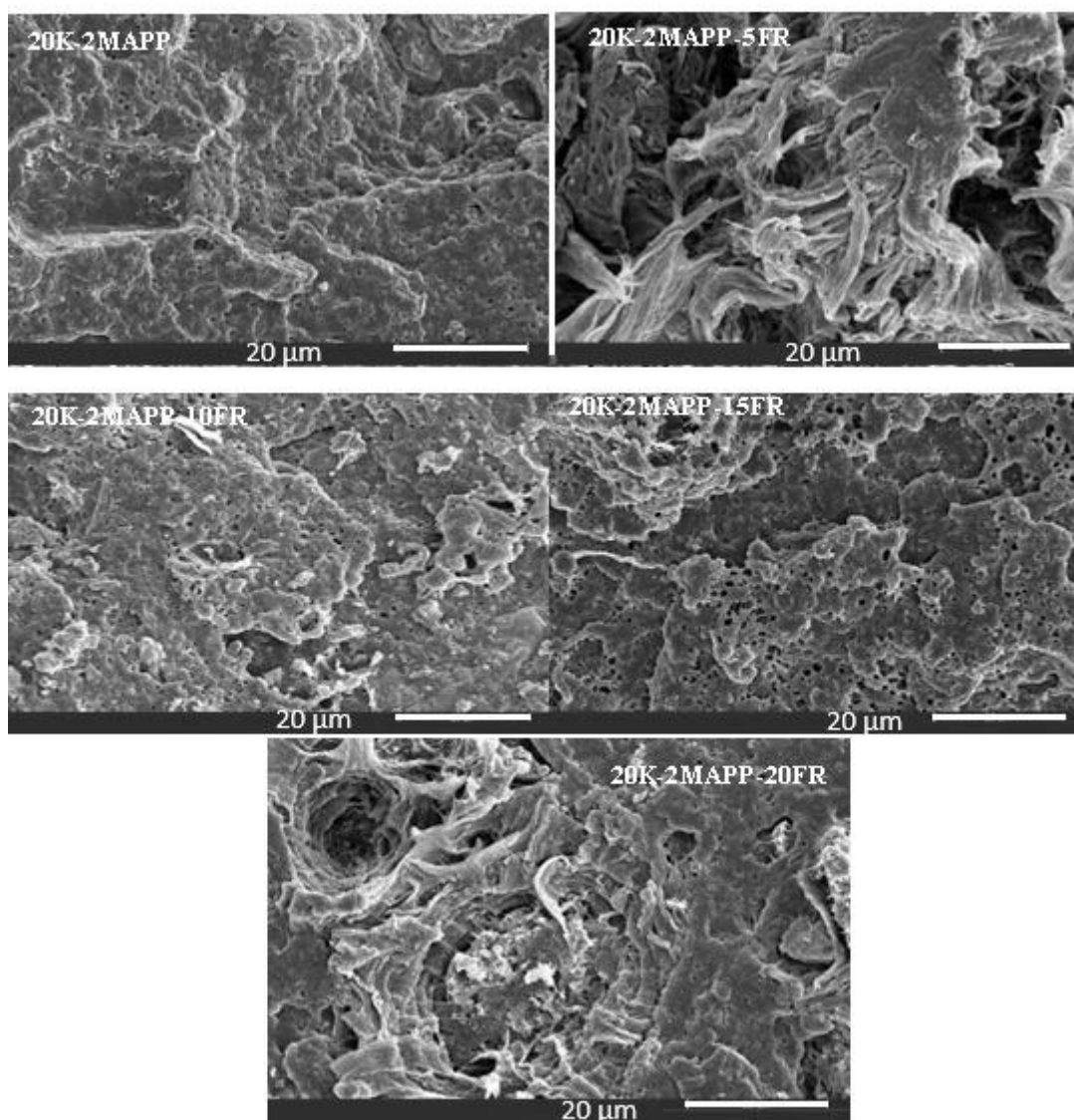


Figure 5. SEM images of FR loaded PP composites.

CONCLUSION

It was found that as the filler ratio increased, the MFI value decreased and the density slightly changed. The lowest mechanical strengths, 13.6 MPa for tensile strength, 24.6 MPa for flexural strength, and 3.3 kJ/m² for impact strength were achieved at a 40% filler ratio. The optimal filler ratio for PP composites was obtained to be 20 wt% after considering mechanical characteristics such as impact strength, tensile and flexural strength, modulus of elasticity, and flexural modulus. Through enhancement of the matrix-filler interface, MAPP considerably increased the mechanical strength of PP composites. However, the notched impact strength of the PP composites was negatively affected by increasing the flame-retardant additive ratio. It was shown that, in the 20K-2MAPP-15FR composite, the burning rate decreased by 42% (relative to the composite without flame retardant (20K-2MAPP)) while the mechanical characteristics were mostly conserved. The burning rate was also found to be

close to PP and was chosen as the optimum combination. This study aims to fill the knowledge gap in the literature by investigating halogen-free flame retardant composites filled with apricot kernel shells, as there are no any studies on this subject. Based on the information gathered here, it was obtained that apricot kernel shell has great potential to replace talc and other conventional inorganic mineral fillers, particularly in the automobile industry. It should be stated that mineral fillers generally provide superior dimensional stability and long-term thermal resistance compared to lignocellulosic fillers. However, apricot kernel shell-filled PP composites offer advantages in sustainability, waste valorization, and potential weight reduction.

REFERENCES

1. Chandramohan D, Murali B, Vasantha-Srinivasan P, Dinesh Kumar S (2019) Mechanical, moisture absorption, and abrasion resistance properties of bamboo–jute–glass fiber composites. *J Bio- Tribo-Corros* 5: 66 [\[CrossRef\]](#)
2. Bhattacharya AB, Chatterjee T, Naskar K (2020) Automotive applications of thermoplastic vulcanizates. *J Appl Polym Sci* 137: 49181 [\[CrossRef\]](#)
3. Izadi M, Bazli L (2025) Eco-friendly composites: developing sustainable solutions for modern engineering. *J Compos Compd* 7(22) [\[CrossRef\]](#)
4. Puttegowda M (2025) Eco-friendly composites: exploring the potential of natural fiber reinforcement. *Discov Appl Sci* 7: 401 [\[CrossRef\]](#)
5. Kamau-Devers K, Miller SA (2020) The environmental attributes of wood fiber composites with bio-based or petroleum-based plastics. *Int J Life Cycle Assess* 25: 1145-1159 [\[CrossRef\]](#)
6. Rivadeneira-Velasco KE, Utreras-Silva CA, Díaz-Barrios A, Sommer-Márquez AE, Tafur JP, Michell RM (2021) Green nanocomposites based on thermoplastic starch: A review. *Polymers* 13: 3227 [\[CrossRef\]](#)
7. Ao X, Vázquez-López A, Mocerino D, González C, Wang D-Y (2024) Flame retardancy and fire mechanical properties for natural fiber/polymer composite: A review. *Compos B Eng* 268: 111069 [\[CrossRef\]](#)
8. Thum MD, Tighe M, Weise NK, Hoffman N, Mosurkal R, Orlicki JA, Lundin JG (2024) Flame-retardant properties and characterization of nylon/tannic acid electrospun fibers. *Adv Eng Mater* 26: 2301333 [\[CrossRef\]](#)
9. Diyana ZN, Jumaidin R, Selamat MZ, Ghazali I, Julmohammad N, Huda N, Ilyas RA (2021) Physical properties of thermoplastic starch derived from natural resources and its blends: A review. *Polymers* 13: 1396 [\[CrossRef\]](#)
10. Sisman M, Teomete E, Yanik J, Malayoglu U, Tac GD (2023) The effects of apricot kernel shell nanobiochar on mechanical properties of cement composites. *Cem Wapno Beton* 28: 2-15 [\[CrossRef\]](#)
11. Yildiz C, Seki Y, Kizilkan E, Sarikanat M, Altay L (2023) Development of halogen-free flame retardant acrylonitrile butadiene styrene (ABS) based composite materials. *ChemistrySelect* 8: e202300989 [\[CrossRef\]](#)
12. Beuguel Q, Boyer SAE, Settipani D, Monge G, Haudin J, Vergnes B, Peuvrel-Disdier E (2018) Crystallization behavior of polypropylene/graphene nanoplatelets composites. *Polym Cryst* 1: e10024 [\[CrossRef\]](#)
13. Bal BC (2023) Some mechanical properties of WPCs with wood flour and walnut shell flour. *Polímeros* 33: e20230020 [\[CrossRef\]](#)

14. Çelik YH, Yalcin R, Topkaya T, Başaran E, Kilickap E (2021) Characterization of hazelnut, pistachio, and apricot kernel shell particles and analysis of their composite properties. *J Nat Fibers* 18: 1054-1068 [\[CrossRef\]](#)
15. Wu P, Liu X, Zhang Z, Wei C (2023) Properties of red mud-filled and modified resin composites. *Constr Build Mater* 409: 133984 [\[CrossRef\]](#)
16. Alshammari BA, Alenad AM, Al-Mubaddel FS, Alharbi AG, Al-shehri AS, Albalwi HA, Alsuabie FM, Fouad H, Mourad AI (2022) Impact of hybrid fillers on the properties of high density polyethylene based composites. *Polymers* 14: 3427 [\[CrossRef\]](#)
17. Erdogan S, Huner U (2018) Physical and mechanical properties of PP composites based on different types of lignocellulosic fillers. *J Wuhan Univ Technol Mater Sci Ed* 33: 1298-1307 [\[CrossRef\]](#)
18. Das A, Satapathy BK (2011) Structural, thermal, mechanical and dynamic mechanical properties of cenosphere filled polypropylene composites. *Mater Des* 32: 1477-1484 [\[CrossRef\]](#)
19. Khalid M, Ratnam C, Chuah T, Ali S, Choong TS (2008) Comparative study of polypropylene composites reinforced with oil palm empty fruit bunch fiber and oil palm derived cellulose. *Mater Des* 29: 173-178 [\[CrossRef\]](#)
20. Pavlík Z, Pavlíková M, Záleská M (2019) Properties of concrete with plastic polypropylene aggregates. In: *Use of recycled plastics in eco-efficient concrete*, Woodhead publishing, pp: 189-213 [\[CrossRef\]](#)
21. Pal T, Pramanik S, Verma KD, Naqvi SZ, Manna P, Kar KK (2022) Fly ash-reinforced polypropylene composites. In: *Handbook of fly ash*, Elsevier, pp: 243-270 [\[CrossRef\]](#)
22. Ayrilmis N, Kaymakci A, Ozdemir F (2013) Physical, mechanical, and thermal properties of polypropylene composites filled with walnut shell flour. *J Ind Eng Chem* 19: 908-914 [\[CrossRef\]](#)
23. Tu Z, Ou H, Ran Y, Xue H, Zhu F (2024) Preparation and flame retardant properties of organic montmorillonite synergistic intumescent flame retardant polypropylene. *J Loss Prev Process Ind* 87: 105226 [\[CrossRef\]](#)
24. Niu D, Yu W, Yang W, Pengwu X, Liu T, Wang Z, Yan X, Ma P (2023) Flame-Retardant and Uv-Shielding Poly (Lactic Acid) Composites with preserved mechanical properties by incorporating cyclophosphazene derivative and phosphorus-modified lignin. *Chem Eng J* 474: 145753 [\[CrossRef\]](#)
25. Lu Y, Wu C, Xu S (2018) Mechanical, thermal and flame retardant properties of magnesium hydroxide filled poly(vinyl chloride) composites: The effect of filler shape. *Compos A: Appl Sci Manuf* 113: 1-11 [\[CrossRef\]](#)
26. Khoshnoud P, Abu-Zahra N (2017) Properties of rigid polyvinyl chloride foam composites reinforced with different shape fillers. *J Thermoplast Compos Mater* 30: 1541-1559 [\[CrossRef\]](#)
27. Deepan S, Jeyakumar R, Mohankumar V, Manojkumar A (2023) Influence of rice husk fillers on mechanical properties of banana/epoxy natural fiber hybrid composites. *Mater Today: Proc* 74: 575-580 [\[CrossRef\]](#)
28. Wang Z, Qiu Y, Liu A, Tang W, Xi W, Wang J, Gao L, Qian L (2023) Micro-crosslinking of phosphaphenanthrene/siloxane molecule initiate aggregation flame retardant and toughening enhancement effects on its polycarbonate composite. *Chem Eng J* 466: 143169 [\[CrossRef\]](#)
29. Dhanola A, Bisht AS, Kumar A, Kumar A (2018) Influence of natural fillers on physico-mechanical properties of luffa cylindrica/ polyester composites. *Mater Today: Proc* 5: 17021-17029 [\[CrossRef\]](#)
30. Sawit PP, Badri KH, Redwan AM (2010) Effect of phosphite loading on the mechanical and fire properties of palm-based polyurethane. *Sains Malays* 39:769-774.
31. Vasanthkumar P, Balasundaram R, Senthilkumar N, Palanikumar K, Lenin K, Deepanraj B (2022) Thermal and thermo-mechanical studies on seashell incorporated Nylon-6 polymer composites. *J Mater Res Technol* 21: 3154-3168 [\[CrossRef\]](#)

32. Asgari M, Masoomi M (2012) Thermal and impact study of PP/PET fibre composites compatibilized with glycidyl methacrylate and maleic anhydride. *Compos B: Eng* 43: 1164-1170 [\[CrossRef\]](#)
33. Stricker F, Bruch M, Mülhaupt R (1997) Mechanical and thermal properties of syndiotactic polypropene filled with glass beads and talcum. *Polymer* 38: 5347-5353 [\[CrossRef\]](#)
34. Nugroho RAA, Alhikami AF, Wang W-C (2023) Thermal decomposition of polypropylene plastics through vacuum pyrolysis. *Energy* 277: 127707 [\[CrossRef\]](#)
35. Nassar MMA, Alzebdeh KI, Al-Hinai N, Safy MA (2024) Enhancing mechanical performance of polypropylene bio-based composites using chemically treated date palm filler. *Ind Crops Prod* 220: 119237 [\[CrossRef\]](#)
36. Sarmin SN, Jawaid M, Ismail AS, Hashem M, Fouad H, Midani M, Salim N (2023) Effect of chitosan filler on the thermal and viscoelasticity properties of bio-epoxy/date palm fiber composites. *Sustain Chem Pharm* 36: 101275 [\[CrossRef\]](#)
37. Chen D, Zheng Q, Liu F, Xu K, Chen M (2010) Flame-retardant polypropylene composites based on magnesium hydroxide modified by phosphorous-containing polymers. *J Thermoplast Compos Mater* 23: 175-192 [\[CrossRef\]](#)
38. Yu M, Chu Y, Xie W, Fang L, Zhang O, Ren M, Sun J (2024) Phosphorus-containing reactive compounds to prepare fire-resistant vinyl resin for composites: Effects of flame retardant structures on properties and mechanisms. *Chem Eng J* 480: 148167 [\[CrossRef\]](#)
39. Pongsa U, Jamesang O, Sangrayub P, Lumsakul P, Kaweejitbundit P, Mookam N (2021) Flammability of short agro-waste pineapple leaf fiber reinforced polypropylene composite modified with diammonium phosphate flame retardant and titanium dioxide. *Fibers Polym* 22: 1743-1753 [\[CrossRef\]](#)
40. Leszczyńska M, Malewska E, Ryszkowska J, Kurańska M, Gloc M, Leszczyński MK, Prociak A (2021) Vegetable fillers and rapeseed oil-based polyol as natural raw materials for the production of rigid polyurethane foams. *Materials* 14: 1772 [\[CrossRef\]](#)
41. Arjmandi R, Hassan A, Majeed K, Zakaria Z (2015) Rice husk filled polymer composites. *Int J Polym Sci* 2015: 501471 [\[CrossRef\]](#)
42. Çavuş V (2020) Selected properties of mahogany wood flour filled polypropylene composites: The effect of maleic anhydride-grafted polypropylene (MAPP). *BioResources* 15: 2227-2236 [\[CrossRef\]](#)
43. Fang L, Lu X, Zeng J, Chen Y, Tang Q (2020) Investigation of the flame-retardant and mechanical properties of bamboo fiber-reinforced polypropylene composites with melamine pyrophosphate and aluminum hypophosphite addition. *Materials* 13: 479 [\[CrossRef\]](#)